

Investigation of morphological, photosynthetic traits, and arbuscular mycorrhizal fungi root infection in sago palm (*Metroxylon sagu* Rottb.) under saline conditions

AIDIL AZHAR^{1*}, LILI DAHLIANI¹, IIS PURNAMAWATI¹, WANDA RUSSIANZI¹, MERRY GLORIA MELIALA¹, FATIMAH NUR ISTIQOMAH^{2,3}, ANDI NUR CAHYO⁴, HIROSHI EHARA^{5,6}

¹Vocational College, IPB University, Bogor, Indonesia

²PT Anugerah Sarana Hayati, Bogor, West Java, Indonesia

³PT Intidaya Agrolestari (INAGRO), West Java, Indonesia

⁴Indonesian Rubber Research Institute, South Sumatera, Indonesia

⁵Graduate School of Bioagricultural Sciences, Nagoya University, Nagoya, Japan

⁶International Center for Research and Education in Agriculture, Nagoya University, Nagoya, Japan

*Corresponding author: aidilazhar@apps.ipb.ac.id

Citation: Azhar A., Dahliani L., Purnamawati I., Russianzi W., Meliala M.G., Istiqomah F.N., Cahyo A.N., Ehara H. (2026): Investigation of morphological, photosynthetic traits, and arbuscular mycorrhizal fungi root infection in sago palm (*Metroxylon sagu* Rottb.) under saline conditions. Hort. Sci. (Prague), 53: 110–118.

Abstract: This study investigated the response of sago palms to saline conditions, focusing on their morphological and photosynthetic performance. The photosynthetic traits were evaluated using OJIP chlorophyll fluorescence transient. The plants were exposed to a saline condition of 224 mM NaCl, and their ability to form associations with arbuscular mycorrhizal fungi (AMF) was also assessed. We tested both commercial AMF products, containing spores from multiple genera, and isolated AMF spores from *Glomus etunicatum* and *Glomus graminicola*, to determine their ability to infect sago palm roots under high salt conditions. The results showed that sago palms can maintain efficient photosynthesis even at high salt levels. This is likely due to their ability to prevent excessive salt uptake in shoots and water loss from roots by forming lignin deposits in cell tissues. Furthermore, the study found that sago palm roots can form associations with AMF under saline conditions. These findings indicate that sago palms exhibit tolerance to saline environments, making them a promising crop option for areas with low soil quality where other carbohydrate-producing crops cannot tolerate the conditions.

Keywords: chlorophyll *a* fluorescence; lignin; saline condition

Plants have evolved mechanisms to cope with environmental stress conditions, including increased soil salinity. Nevertheless, soil salinity poses significant challenges to the growth of terrestrial plants. Research has shown that even moderate increases in soil salinity, around 40 mM NaCl, can disrupt plant growth due to osmotic stress caused by elevated sodium (Na⁺) and chloride (Cl⁻) ions (Julkowska, Testerink 2015; Munns, Gilliam 2015; Byrt et al. 2018).

Soil salinity can lead to reduced crop yields by inhibiting leaf photosynthesis. This inhibition occurs due to the inactivation of photosystem II (PSII) reaction centres, caused by electron transport disruption (Çiçek et al. 2018). Additionally, increased salinity triggers the release of abscisic acid (ABA) in guard cells, leading to stomatal closure (Geilfus et al. 2015; Hniličková et al. 2017). This closure is further exacerbated by short-term alkalinisation

<https://doi.org/10.17221/26/2025-HORTSCI>

of the apoplast (Geilfus 2017), resulting in osmotic effects that activate enzymes involved in carbon dioxide (CO₂) reduction (Xu, Zhou 2008), ultimately affecting the carbon reduction cycle.

Saline conditions can occur naturally, arising from underground sources or the use of brackish irrigation water. However, unsustainable land clearing and irrigation practices have exacerbated the problem, particularly when marginal lands are converted into agricultural and plantation production areas. To mitigate the impact of saline soils on global carbohydrate production, researchers are exploring agronomic solutions. One approach is to cultivate carbohydrate-rich plant species that are tolerant of saline conditions.

Cultivating sago palm (*Metroxylon sagu* Rottb.) on saline soils affected by brackish water is a potential agronomic solution for utilising marginal lands to support global carbohydrate production. Sago palm, a high-starch plant species, exhibits high adaptability to grow in marginal lands, including peatlands and saline areas, without requiring special cultivation treatments like fertiliser applications (Ehara 2005; Azhar et al. 2020). Soil microorganisms, such as arbuscular mycorrhizal fungi (AMF), play a crucial role in facilitating the availability of soil nutrients, particularly phosphate, for sago palm growth. A previous study found that various AMF species in Thai sago palm habitats infect sago palm

roots growing on peatlands. However, the impact of saline conditions due to brackish water on AMF colonisation and infection in sago palm roots remains unreported.

This study explores how sago palms respond to saline conditions, examining their morphological and photosynthetic traits using OJIP chlorophyll fluorescence transient methods. The goal is to understand the strategies sago palms use to thrive in saline environments. Additionally, the study investigates how AMF infect sago palm roots under saline conditions.

MATERIAL AND METHODS

This experiment was conducted in a greenhouse of PT INAGRO in West Java, Bogor Regency, Indonesia. Four-month-old sago palm seedlings were transplanted individually from a 473 mL plastic cup into a 30 × 30 cm polybag filled with medium size zeolite as the growing medium. During transplanting, 5 g of zeolite containing spores of AMF were added to the seedlings in the experimental plots. The AMF spores came from three sources: *Glomus etunicatum*, *Glomus grape*, and a commercial AMF fertiliser called MZ2000. The MZ2000 fertiliser contains a mix of spores from *Glomus grape*, *Glomus manihotis*, *Glomus etunicatum*, and *Acaulospora*, as shown in the photomicrograph in Figure 1.

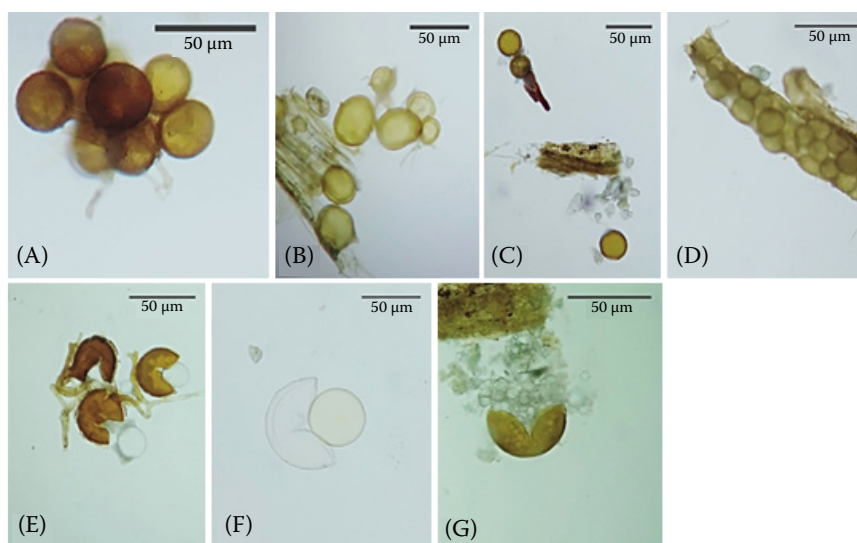


Figure 1. Arbuscular mycorrhizal fungi (AMF) spore of (A) *Glomus grape*, (B) *Glomus manihotis*, (C) *Glomus etunicatum*, (D) *Acaulospora*, (E) crashed *Glomus grape*, (F) crashed *Glomus manihotis*, and (G) crashed *Glomus etunicatum* contained in MZ2000 (commercial mycorrhizal fertiliser)

<https://doi.org/10.17221/26/2025-HORTSCI>

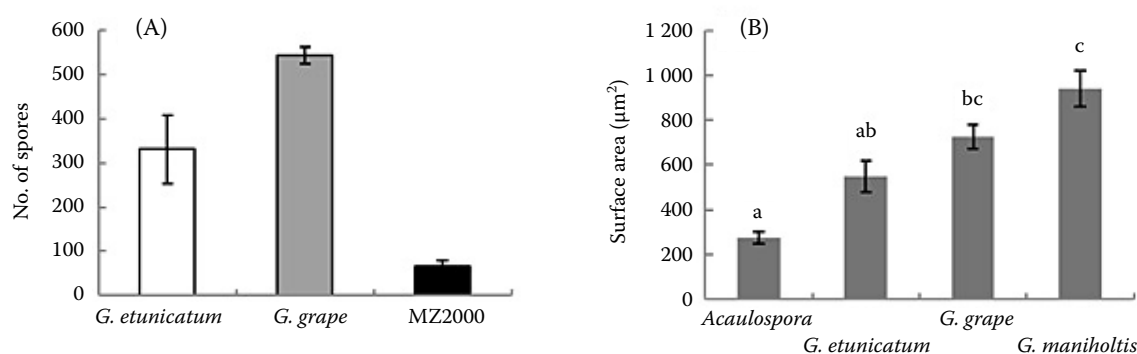


Figure 2. (A) Number of spores from 5 g isolated mycorrhizal inocula from *Glomus etunicatum*, *Glomus grape*, and commercial mycorrhizal inocula MZ2000 (commercial mycorrhizal fertiliser) which consisted of *Acaulospora*, and *Glomus maniholtis* ($n = 6$), (B) surface area of different arbuscular mycorrhizal fungi (AMF) spores ($n = 4$) Data correspond to the mean value and standard error ($n = 4$); ^{a,b,c} different letters indicate significant difference at the $P < 0.001$ level for each according to Tukey honest significant difference

Figure 2 shows the species and number of AMF spores present in 5 g of zeolite. All the seedlings were placed into a plastic bucket filled with Kimura-B culture solution up to half part of the polybag (root zone) submerged with water. After two months, the sago palm seedlings were exposed to Kimura-B culture solution mixed with 224 mM NaCl for salinity treatment for two months. There was no NaCl treatment for the control plots.

The sago palm morphological traits. Observations of plant morphological traits, such as plant height and leaflet area, were taken every two weeks from the beginning to the end of the experiment. Plant height was measured from the base of the trunk to the tip of the longest leaf. Leaflet area was measured by photographing each leaf from each plant sample and analysing the images using ImageJ software (version 1.0, 1997). At the end of the experiment, the dry matter weight of leaves and roots was measured after drying all plant biomass in an oven at 70 °C for four days. Leaf greenness was measured at the second leaf position from the top using a chlorophyll meter (SPAD-502Plus, Konica Minolta, Japan).

Lignin deposition in the roots. The main and secondary roots of the seedlings from each treatment were collected for lignin analysis. A cross-section of the roots was soaked in a clearing solution containing chloral hydrate, glycerin, and milli-Q water for an hour. Next, the root cross-section was placed on a microscope slide and stained with 3% phloroglucinol for 10 minutes. The sample was then treated with 6N HCl before being examined

under a microscope. The resulting pink coloration of the root tissue indicated lignin deposition.

AMF infection in the roots. Fine root samples were collected from the control and 224 mM NaCl treatment plots of *Glomus etunicatum*, *Glomus grape*, and MZ2000 ($n = 4$) to assess the status of AMF infection. All root samples were washed and then soaked in a 10% KOH solution for two days, until the root colour became clear. After soaking, the roots were thoroughly cleaned to remove the KOH solution. Next, the root samples were dipped in a 2% HCl solution. The roots were then immersed in a staining solution for 6–24 hours. The staining solution consisted of 0.5 mL of trypan blue diluted with 200 mL of distilled water, 400 mL of glycerin, and 400 mL of lactic acid. Finally, root infection by AMF was observed under a microscope.

Leaf chlorophyll fluorescence. Chlorophyll fluorescence measurements were taken between 9:00 and 12:00 to assess the photosynthetic performance of sago palms under saline conditions. Using a portable fluorometer (Pocket PEA, Hansatech Instruments Ltd., Norfolk, England), O-J-I-P fluorescence transients were recorded at the end of the experiment. Leaf samples were taken from the second leaf position from the top of the branch. To ensure dark adaptation, the middle portion of the leaf's adaxial surface was covered with a leaf clip provided by Hansatech Instruments for at least 20 minutes. A saturation pulse of 3 000 μmol was then applied to the leaf to induce maximum fluorescence (F_m).

<https://doi.org/10.17221/26/2025-HORTSCI>

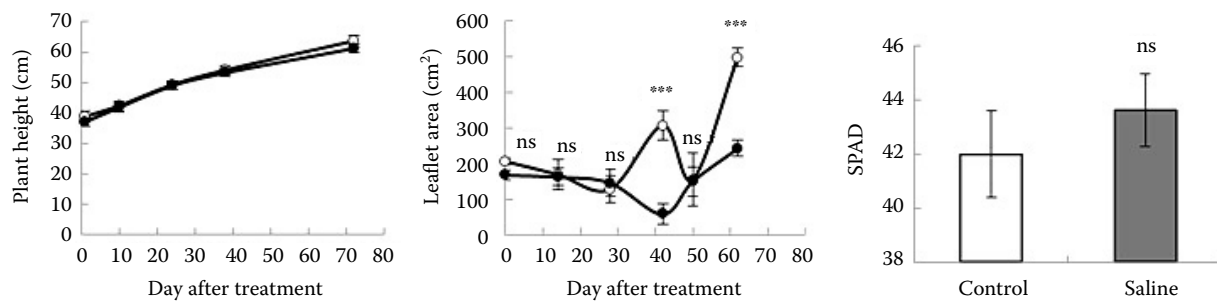


Figure 3. The trend of plant height, new developed leaflet area, and leaves greenness (SPAD), of sago palm under normal (○) and saline conditions (■)

***significant levels at the 0.001 probability level, respectively, according to Student's *t*-test; data correspond to the mean value and standard error ($n = 20$); ns – not significant

RESULTS

Two months of salt treatment did not significantly impact the height of sago palm seedlings. However, salt stress significantly affected the emergence of new leaves. Under salt stress, sago palms exhibited slower leaf growth, as evidenced by lower leaflet area values (Figure 3).

Interestingly, salt stress did not affect leaf greenness, with no significant difference in SPAD values between treatments. Visual observations of leaf greenness are shown in Figure 4.

Although the SPAD values did not differ significantly between treatments, a trend emerged where the SPAD values were higher in sago palms treated with 224 mM NaCl than in the control plot without NaCl treatment.

Sago palm seedlings treated with 224 mM NaCl exhibited lignin deposition in their roots. The presence of lignin in root tissues is evident from the red staining observed in cross-sections of both main and secondary roots. In main root cross-sections, high lignin formation was observed in the exocarp tissue, extending to the outer layer of the cortex tissue (Figures 5B and 5D). Lignin also covered the stele area, which includes endodermis, pith, and vascular tissues such as phloem and xylem.

Salt stress caused rapid death of cortex tissues, as indicated by dark coloration, particularly in the inner layer adjacent to the stele and the middle layer, leading to increased aerenchyma formation. Similar lignin deposition was observed in cross-sections of secondary roots (Figure 5E). In contrast, cross-sections of sago palm roots grown in the control plot without NaCl treatment (Figure 5A and 5C) showed no red coloration, indicating negligible lignin deposition.

The 224 mM NaCl treatment also had a detrimental effect on the root growth of sago palm seedlings (Figure 6). Under saline conditions, root growth was inhibited, leading to rapid root mortality, as evidenced by the darker, rotten root colour. In contrast, sago palm seedlings grown under non-saline conditions exhibited robust root growth. Additionally, saline conditions accelerated necrosis and increased mortality in older leaves, particularly those located in lower positions (Figure 4).



Figure 4. The saline condition reduced root growth and enhanced leaf necrosis in the lower leaf positions (older leaves) specified by the black arrows

The middle and uppermost leaves were not affected by the saline conditions

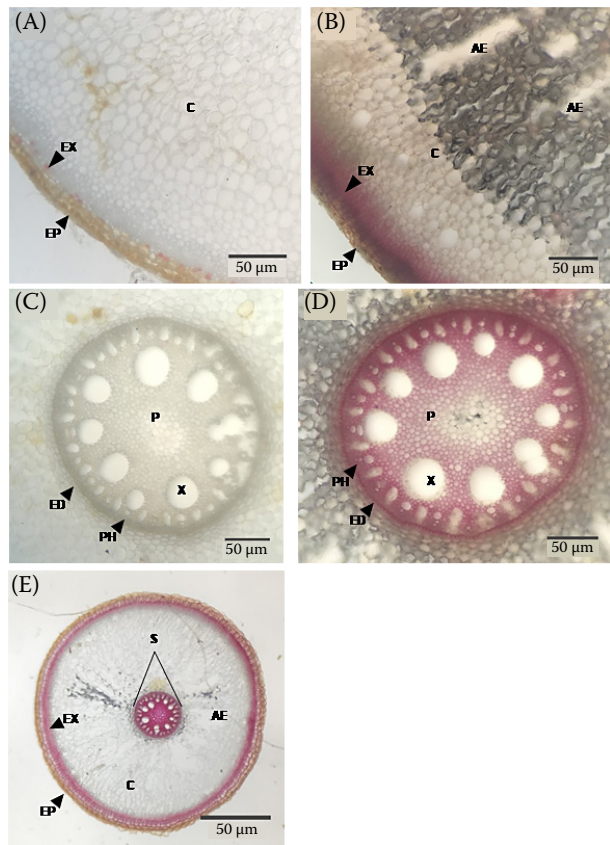


Figure 5. Sago palm main root cross sections grown under (A) and (C) normal and (B) and (D) saline conditions and (E) secondary root cross section under saline conditions EP – epidermis; EX – exodermis; C – cortex; AE – aerenchyma; S – stele; ED – endodermis; PH – phloem; X – xylem; P – pith; red colour in root tissues indicate lignin deposition under saline conditions

The leaf photosynthetic efficiency of sago palm seedlings remained unaffected by the 224 mM NaCl treatment. After two months of exposure to saline conditions, the plants maintained efficient light energy utilisation for photochemical quenching. This was confirmed by the chlorophyll fluorescence transient data of the O-J-I-P steps in Figure 7.

Under saline conditions, the fluorescence intensity of the O-J and J-I steps was lower than in the non-saline treatment. The OJIP steps parameters in Table 1 show that, under saline conditions, plants utilised light energy more efficiently, as indicated by lower values of minimum fluorescence (F_0), I-step fluorescence (F_1), and J-step fluorescence (F_j), compared to the non-saline treatment (control). Additionally, the lower values of specific energy flux per reaction centre, such as absorption per reac-

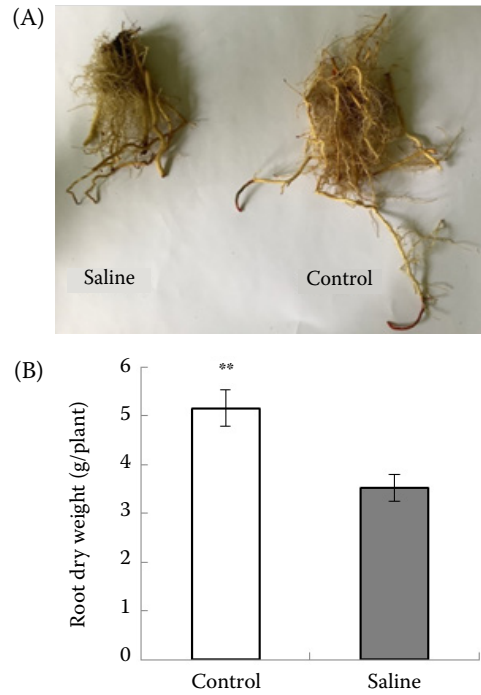


Figure 6. (A) Sago palm roots grown under normal (control) and saline conditions and (B) root dry matter weight under control and saline condition

**significantly different at 1% according to the Student's *t*-test ($n = 20$)

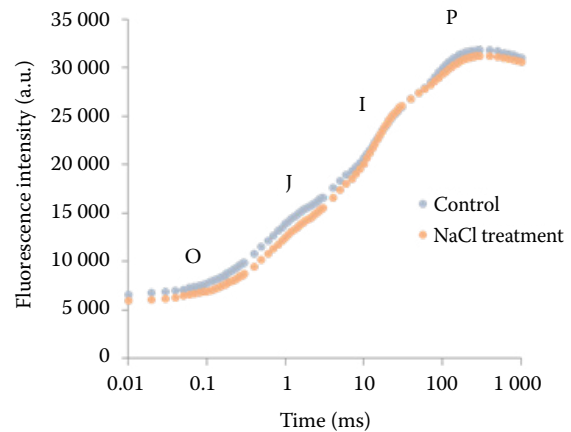


Figure 7. Chlorophyll *a* fluorescence curves (OJIP transients) of sago palm leaves

O-J-I-P indicate the specific steps in the chlorophyll *a* fluorescence transient of sago palm leaf grown under normal and saline conditions

tion center (ABS/RC), trapping per RC (TRo/RC), electron transport per RC (ETo/RC), dissipation per RC (DIo/RC), and reduction of end electron acceptors per RC (REo/RC), along with a higher

<https://doi.org/10.17221/26/2025-HORTSCI>

Table 1. Comparison of OJIP steps in response to saline conditions

Treatment	Area	F _o	F _J	F _I	F _M
Control	637 515 ± 23 325 ^{ns}	6 403 ± 117 ^{**}	8 847 ± 167 ^{***}	16 514 ± 315 [*]	31 306 ± 510 ^{ns}
Saline	635 747 ± 20 072	6 032 ± 115	8 029 ± 106	15 239 ± 413	31 464 ± 484

F_o – minimum fluorescence; F_J – J-step fluorescence; F_I – I-step fluorescence; F_M – maximum fluorescence; *, **, ***significantly different at $P < 0.05, 0.01$ and 0.001 , respectively, according to the Student t -test ($n = 20$); ns – non-significant

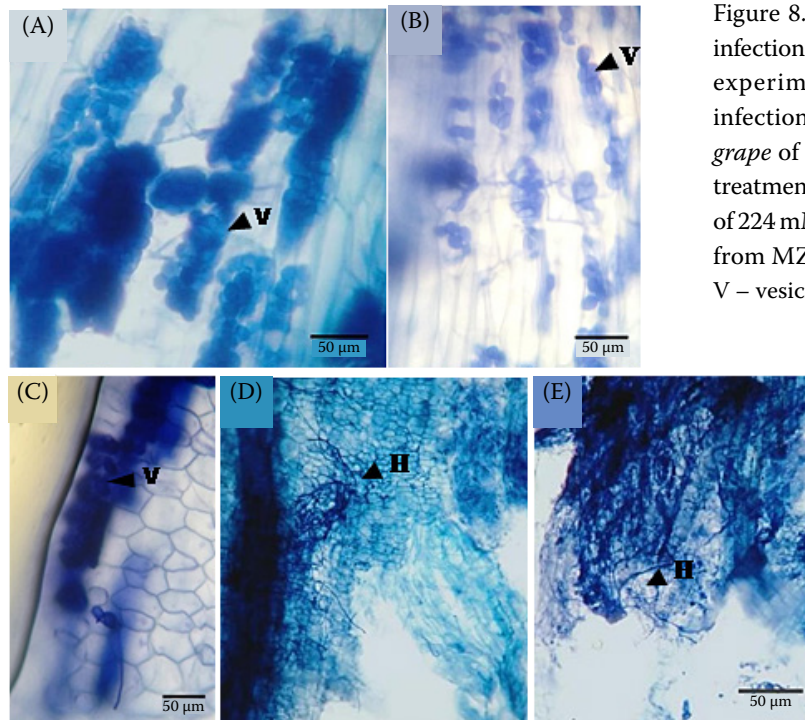


Figure 8. The arbuscular mycorrhizal fungi (AMF) infection was found in the *Glomus grape* and MZ2000 experimental plots; photomicrograph of AMF infection in the root samples taken from *Glomus grape* of the control (A) and (B) and 224 mM NaCl treatment plots (C); AMF hyphae from *Glomus grape* of 224 mM NaCl treatment plot (D) and AMF hyphae from MZ2000 the control plot (E)
V – vesicle; H – hyphae

performance index on absorption basis (PI_{ABS}), further confirmed the improved light energy utilisation for photochemical quenching under NaCl treatment (Table 2).

Figure 8 shows photomicrographs of AMF-infected sago palm roots in the experimental plots of *Glomus grape* under control (Figures 8A, B) and 224 mM NaCl treatment (Figure 8C).

The infection is evident from the presence of numerous vesicles, resembling grape clusters, and hyphae within the sago root tissue (Figure 8D). In contrast, no infection was observed in the plots of *Glomus etunicatum*. However, hyphae were detected in the control plot of MZ2000 (Figure 8E).

DISCUSSION

High levels of sodium can severely impede enzyme function in plants, while also disrupting

the absorption of vital nutrients such as calcium, potassium, and zinc (Iqbal et al. 2018; Wu et al.

Table 2. Specific energy flux per reaction centre and the performance index of sago palm under normal and saline conditions

Parameters	Control	Saline condition
ABS/RC	15 781	13 792.05 ^{***}
TRo/RC	12 541	10 148 ^{**}
ETo/RC	0.79	0.74 ^{**}
DIo/RC	0.32	0.27 ^{***}
REo/RC	0.29	0.23 ^{***}
PI _{ABS}	4 370	6 236 ^{***}

ABS – absorption; RC – reaction center; TRo – trapping; ETo – electron transport; DIo – dissipation; REo – reduction of end electron acceptors; PI_{ABS} – absorption basis; **, ***significantly different at $P < 0.01, 0.001$, respectively, according to the Student t -test ($n = 20$)

2018; Zhang et al. 2023). Prolonged exposure to salt stress triggers a surge in the production of reactive oxygen species (ROS) within plants, potentially stunting growth and development, and in extreme cases, causing plant mortality (Singh et al. 2016).

According to the data revealed in this study, it can be considered that the sago palm can survive growing in high NaCl concentrations, such as 224 mM NaCl concentration for a particular time tested. The plant adopted a salt avoidance mechanism to prevent the high salt concentration was transported to the source organs, such as leaves. Previous studies reported that under saline conditions, the plants mainly store high concentrations of Na⁺ in the roots and petioles and low Na⁺ concentrations in active leaflets. It was also reported that the leaf gas exchange was reduced by up to 40% under salt-stress conditions (Prathumyot et al. 2011). Although the leaf gas exchange of the sago palm was decreased by 40%, in this study, we found that the salt stress did not affect the sago palm leaf photosynthetic efficiency. Under the saline condition, the efficiency in using light energy for photochemical quenching was maintained well, even higher under salt stress.

Saline conditions enhanced the utilisation of light energy, as evident in the OJIP fluorescence transients (Table 1). The sago palm demonstrated improved photosynthetic efficiency under saline conditions compared to the control (Figure 6 and Table 2). The rise in the O-J phase of fluorescence following NaCl treatment indicates that some PSII reaction centres remain open, facilitating enhanced electron transport on the acceptor side of PSII (Strasser et al. 2004; Kalaji et al. 2016; Azhar et al. 2023). This increase is attributed to elevated levels of the primary plastoquinone electron acceptor of PSII (Q_A) in photosystem II (Strasser et al. 2004). Furthermore, the J-I phase of fluorescence showed a lower trend under NaCl treatment, indicating normal functioning of secondary electron acceptors, including Q_B, plastoquinone (PQ), cytochrome (Cyt b6f), and plastocyanin (PC) (Guha et al. 2013). The lower I-P phase in NaCl treatment suggests optimal electron transport in photosystem I (PSI), involving electron transporters such as ferredoxin, intermediary acceptors, and NADP.

Exposure to NaCl did not affect the sago palm's OJIP curve area, indicating normal electron transfer from the reaction centre (RC) to the quinone pool (Kumar et al. 2020). This area reflects the

pool size of electron acceptors Q_A on the reducing side of PSII. Under saline conditions, specific energy flux per reaction centre (ABS/RC, TR_O/RC, ET_O/RC, and DI_O/RC) significantly lower than control, suggesting normal or more efficient in light photochemical quenching.

According to Yang et al. (2016), chlorophyll fluorescence reveals photosynthetic function. Higher ABS/RC values indicate increased antenna size, while high TR_O/RC values suggest RC transformation (Schansker, Strasser 2005) due to electron transport inhibition from Q_A to Q_B (Yusuf et al. 2010) and oxygen-evolving complex inactivation (Liang et al. 2019) or impairment (Braga et al. 2020). Elevated ET_O/RC and DI_O/RC values indicate excess light energy dissipation to minimise photodamage (Akhter et al. 2021). These changes led to a significant decrease in the performance index on an absorption basis (PI_{ABS}). However, this study surprisingly found a significant increase in the sago palm's performance index under saline conditions, despite no increase in specific energy flux per reaction centre.

The success of sago palm in maintaining optimum light energy utilization under saline conditions can be attributed to its roots' ability to barrier excess sodium uptake from the soil. This is facilitated by the roots' capacity to produce lignin in root tissues. Lignin, primarily found in the secondary cell wall, provides structural support and physical strength to plants, and facilitates water and mineral transport through the xylem (Choi et al. 2023). Under NaCl stress, sago roots accumulate high levels of lignin in the exodermis, endodermis, and stele tissues, as indicated by intense red staining (Figure 7). This lignin formation prevents excessive sodium transport, excluding salt from the shoot (Naseer et al. 2012) and protecting photosynthetically active leaves from sodium toxicity. However, salt stress has a detrimental effect on sago root growth, particularly affecting the secondary roots (those greater than 2 mm in diameter). Research on various plant species, including *Arabidopsis* (Chun et al. 2019), wheat (Riaz et al. 2023), rice (Xue et al. 2024), barley (Ho et al. 2020), soybean (Cai et al. 2022), and oil palm (Govender et al. 2020), has shown that salt and drought stress trigger increased root lignification, strengthening cell walls and limiting sodium ion entry into the root xylem.

This study investigated the potential for AMF to infect sago roots under saline conditions. The

<https://doi.org/10.17221/26/2025-HORTSCI>

results showed that while the infection rate was low, AMF infection in sago roots is still possible even in saline environments. Research has demonstrated that AMF can help mitigate the damaging effects of salt stress on plants (Zhang et al. 2023).

Microscopic analysis revealed that under saline conditions, the hyphae and vesicles of AMF were visibly present (Figure 8). Notably, AMF vesicles can sequester ions like Na^+ and Cl^- , thereby enhancing plant tolerance to salt stress by reducing ion uptake through the roots (Ait-El-Mokhtar et al. 2020; Miransari 2010). However, the impact of saline conditions on AMF is complex and depends on various factors. Some studies have reported that saline conditions can inhibit AMF spore germination and hinder hyphal growth, particularly at high NaCl concentrations at 150 mM (Heikam et al. 2009). On the other hand, other research has found that saline conditions can increase AMF spore production and colonisation in certain cases (Aliasgharzadeh et al. 2001). For instance, Yamato et al. (2008) discovered that AMF colonisation rates in coastal vegetation on Okinawa Island remained unaffected by 200 mM NaCl treatments.

To further advance this research, it is essential to identify specific AMF species that are tolerant of saline conditions and compatible with sago palm roots. Another potential approach is to use compound inoculants containing multiple AMF species, as demonstrated in a previous study on rice plants (Zhang et al. 2023).

CONCLUSION

This study reveals three key findings. Firstly, sago palms can efficiently utilize light energy for photochemical quenching, even when exposed to high salinity levels of 224 mM NaCl. Secondly, the plant's ability to maintain efficient photosynthetic performance under saline conditions may be attributed to its avoidance mechanism, which prevents excessive sodium uptake in shoots and water loss from roots by forming lignin deposits in tissues. Thirdly, the study suggests that sago palm roots can be infected with AMF under saline conditions. However, further research is needed to identify specific AMF species that are tolerant of saline conditions and compatible with sago palm roots.

Acknowledgement: The authors thank PT Intidaya Agrolestari (INAGRO) and the team members for their support in this experiment.

REFERENCES

- Akhter N., Ashraf M., Akram N.A., Al-Qurainy F., Shafiq S. (2021): Role of chlorophyll fluorescence in assessing photosynthetic performance under abiotic stress conditions. *Journal of Plant Growth Regulation*, 40: 158–172.
- Aliasgharzadeh N., Saleh R.N., Towfighi H., Alizadeh A. (2001): Occurrence of arbuscular mycorrhizal fungi in saline soils of the Tabriz Plain of Iran in relation to some physical and chemical properties of soil. *Mycorrhiza*, 11: 119–122.
- Ait-El-Mokhtar M., Baslam M., Ben-Laouane R., Anli M., Boutasknit A., Mitsui T. (2020): Alleviation of detrimental effects of salt stress on date palm (*Phoenix dactylifera* L.) by the application of arbuscular mycorrhizal fungi and/or compost. *Frontier Sustainable Food Systems*, 4: 131.
- Azhar A., Makihara D., Naito H., Ehara H. (2020): Evaluating sago palm (*Metroxylon sagu* Rottb.) photosynthetic performance in waterlogged conditions: Utilizing pulse-amplitude-modulated (PAM) fluorometry as a waterlogging stress indicator. *Journal of the Saudi Society of Agricultural Sciences*, 19: 37–42.
- Azhar A., Merdekawati E., Pramudia A., Cahyo A.N., Ehara H., Dahliani L. (2023): Ambient air temperatures and solar radiation affect OJIP fluorescence transients of coffee plants in an agroforestry system. *Agrosystems, Geosciences, and Environment*, 6: e20340.
- Braga K., Batista P.F., de Carvalho F.E.L., Nascimento K.J.T., Silveira J.A.G. (2020): Salt stress leads to photoinhibition by disrupting photosystem II and oxygen-evolving complex in plants. *Environmental and Experimental Botany*, 178: 104156.
- Byrt C.S., Munns R., Burton R.A., Gilliam M., Wege S. (2018): Root cell wall solutions for crop plants in saline soils. *Plant Science*, 269: 47–55.
- Cai X., Jia B., Sun M., Sun X. (2022): Insights into the regulation of wild soybean tolerance to salt-alkaline stress. *Frontiers in Plant Science*, 13: 1002302.
- Choi S.J., Lee Z., Kim S., Jeong E., Shim J.S. (2023): Modulation of lignin biosynthesis for drought tolerance in plants. *Frontiers in Plant Science*, 14: 1116426.
- Chun S.C., Paramasivan M., Chandrasekaran M. (2019): Proline accumulation influenced by osmotic stress in *Arabidopsis thaliana*. *Frontiers in Plant Science*, 10: 1–10.
- Çiçek N., Oukarroum A., Strasser R.J., Schansker G. (2018): Salt stress effects on the photosynthetic electron transport chain in two chickpea lines differing in their salt stress tolerance. *Photosynthesis Research*, 136: 291–301.
- Ehara H. (2005): Geographical distribution and specification of *Metroxylon palms*. *Japanese Journal of Tropical Agriculture*, 50: 229–233.
- Geilfus C.M. (2017): The pH of the apoplast: Dynamic factor with functional impact under stress. *Molecular Plant*, 10: 1371–1386.

<https://doi.org/10.17221/26/2025-HORTSCI>

- Geilfus C.M., Mithofer A., Muller J.L., Zorb C., Muehling K.H. (2015): Chloride-inducible transient apoplastic alkalizations induce stomata closure by controlling abscisic acid distribution between leaf apoplast and guard cells in salt-stressed *Vicia faba*. *New Phytologist*, 208: 803–816.
- Govender N., Seman I.A., Yun W.M. (2020): Root lignin composition and content in oil palm (*Elaeis guineensis* Jacq.) genotypes with different defense responses to *Ganoderma boninense*. *Agronomy*, 10: 1487.
- Guha A., Sengupta D., Reddy A.R. (2013): Polyphasic chlorophyll a fluorescence kinetics and leaf protein analyses to track dynamics of photosynthetic performance in mulberry during progressive drought stress. *Journal of Photochemistry and Photobiology B: Biology*, 119: 71–83.
- Heikam E., Kapoor R., Giri B. (2009): Arbuscular mycorrhizal fungi in alleviation of salt stress: A review. *Annals of Botany*, 104: 1263–1280.
- Hniličková H., Hnilička F., Martinková J., Kraus K. (2017): Effects of salt stress on water status, photosynthesis and chlorophyll fluorescence of rocket. *Plant Soil Environment*, 63: 362–367.
- Ho C.H., Lin S.H., Hu H.C., Tsay Y.F. (2020): CHL1 functions as a nitrate sensor in plants. *Cell*, 138: 1184–1194.
- Iqbal M.N., Rasheed R., Ashraf M.Y., Ashraf M.A., Hussain I. (2018): Exogenously applied zinc and copper mitigate salinity effect in maize (*Zea mays* L) by improving key physiological and biochemical attributes. *Environmental Science and Pollution Research*, 25: 23883–23896.
- Julkowska M.M., Testerink C. (2015): Tuning plant signaling and growth to survive salt. *Trends in Plant Science*, 20: 586–594.
- Kalaji H.M., Jajoo A., Oukarroum A., Brestic M., Zivcak M., Samborska I.A., Cetner M.D., Łukasik I., Goltsev V., Ladle R.J. (2016): Chlorophyll a fluorescence as a tool to monitor physiological status of plants under abiotic stress conditions. *Acta Physiologiae Plantarum*, 38: 102.
- Kumar D., Yusuf M.A., Singh P., Sardar M., Sarin N.B. (2020): Histochemical detection of superoxide and hydrogen peroxide accumulation in *Brassica juncea* seedlings. *Bio-Protocol*, 10: e3525.
- Liang Y., Cheng X., Zhao T., Zhang X., Wang Y. (2019): Effects of abiotic stress on photosystem II and oxygen-evolving complex in plants. *Photosynthetica*, 57: 123–132.
- Miransari M. (2010): Contribution of arbuscular mycorrhizal symbiosis to plant growth under different types of soil stress. *Plant Biology*, 12: 563–569.
- Munns R., Gilliam M. (2015): Salinity tolerance of crops – What is the cost? *New Phytologist*, 208: 668–673.
- Naseer S., Lee Y., Lapierre C., Franke R., Nawrath C., Geldner N. (2012): Casparian strip diffusion barrier in *Arabidopsis* is made of a lignin polymer without suberin. *The Proceedings of the National Academy of Sciences*, 109: 10101–10106.
- Prathumyot W., Ehara H., Yamauchi A. (2011): Physiological responses of sago palm (*Metroxylon sagu* Rottb.) to salinity stress: Ion distribution and leaf gas exchange. *Tropical Agriculture and Development*, 55: 91–97.
- Riaz M.W., Yousaf M.I., Hussain Q., Yasir M., Sajjad M., Shah L. (2023): Role of lignin in wheat plant for the enhancement of resistance against lodging and biotic and abiotic stresses. *Stresses*, 3: 434–453.
- Schansker G., Strasser R.J. (2005): Quantification of non-Q_B-reducing centers in leaves using a far-red pre-illumination. *Photosynthesis Research*, 84: 145–151.
- Singh R., Singh S., Parihar P., Mishra R.K., Tripathi D.K., Singh V.P., Chauhan D.K., Prasad S.M. (2016): Reactive oxygen species (ROS): Beneficial companions of plants' developmental processes. *Frontiers in Plant Science*, 7: 1299.
- Strasser R.J., Tsimilli-Michael M., Srivastava A. (2004): Analysis of the chlorophyll a fluorescence transient. In: Papageorgiou G.C., Govindjee (eds): *Chlorophyll a Fluorescence. Advances in Photosynthesis and Respiration*. Dordrecht, Springer: 321–362.
- Wu H., Zhang X., Giraldo J.P., Shabala S. (2018): It is not all about sodium: Revealing tissue specificity and signalling roles of potassium in plant responses to salt stress. *Plant and Soil*, 431: 1–17.
- Xu Z., Zhou G. (2008): Responses of leaf stomatal density to water status and its relationship with photosynthesis in a grass. *Journal of Experimental Botany*, 59: 3317–3325.
- Xue B., Duan W., Gong L., Zhu D., Li X., Li X. (2024): The *OsDIR55* gene increases salt tolerance by altering the root diffusion barrier. *The Plant Journal*, 118: 1550–1568.
- Yamato M., Ikeda S., Iwase K. (2008): Community of arbuscular mycorrhizal fungi in coastal vegetation on Okinawa Island and effect of the isolated fungi on growth of sorghum under salt-treated conditions. *Mycorrhiza*, 18: 241–249.
- Yang H., Yang X., Zhang Y., Heskell M.A., Lu X., Munger J.W., Sun S., Tang J. (2016): Chlorophyll fluorescence tracks seasonal variations of photosynthesis from leaf to canopy in a temperate forest. *Global Change Biology*, 23: 2874–2886.
- Yusuf M.A., Kumar D., Rajwanshi R., Strasser R.J., Tsimilli-Michael M., Sarin N.B. (2010): Overexpression of γ -tocopherol methyl transferase gene in transgenic *Brassica juncea* plants alleviates abiotic stress: Physiological and chlorophyll fluorescence analysis. *Biochimica et Biophysica Acta*, 1797: 1428–1438.
- Zhang B., Shi F., Zheng X., Pan H., Wen Y., Song F. (2023): Effects of AMF compound inoculants on growth, ion homeostasis, and salt tolerance-related gene expression in *Oryza sativa* L. under salt treatments. *Rice*, 16: 18.

Received: February 25, 2025

Accepted: September 24, 2025

Publish online: April 9, 2026